AIChE

Natural Rectorite Mineral: A Promising Substitute of Kaolin for In-Situ Synthesis of Fluid Catalytic Cracking Catalysts

Baoying Wei, Haiyan Liu, Tiesen Li, Liyuan Cao, and Yu Fan
State Key Laboratory of Heavy Oil Processing, China University of Petroleum, Changping, Beijing 102249, P. R. China

Xiaojun Bao
State Key Laboratory of Heavy Oil Processing, China University of Petroleum, Changping, Beijing 102249, P. R. China; and The Key Laboratory of Catalysis, China National Petroleum Corporation, China University of Petroleum, Changping, Beijing 102249, P. R. China

DOI 10.1002/aic.12195
Published online June 1, 2010 in Wiley Online Library (wileyonlinelibrary.com).

Fabrication of high-performance fluid catalytic cracking (FCC) catalysts is suffering from the shortage of high-quality kaolin that has long been used as matrix or starting material for synthesizing FCC catalysts. This work aimed at exploring the potential of rectorite, a natural aluminosilicate mineral, to substitute kaolin for preparing FCC catalysts through in-situ synthesis technique. The physicochemical properties of a rectorite mineral, including its chemical composition, structure, thermal behavior, and chemical reactivity, were systemically investigated and compared with those of commercial kaolin. The results showed that the rectorite mineral suitably treated could substitute kaolin for synthesizing FCC catalysts. Moreover, we had shown that a hydrothermally stable ZSM-5/rectorite composite in which ZSM-5 crystals of ca. 2 μm in size were overgrown on preformed rectorite substrate could be synthesized using the rectorite mineral calcined at 800°C as raw material. When used as FCC additive, the obtained ZSM-5/rectorite composite demonstrated enhanced light olefin (ethylene and propylene) yields. © 2010 American Institute of Chemical Engineers *AIChE J,* 56: 2913–2922, 2010

Keywords: rectorite mineral, FCC catalyst, in-situ synthesis

Introduction

In the modern petroleum refining industry, fluid catalytic cracking (FCC) is the most important process converting heavy feedstocks into lighter vehicle fuels such as gasoline and diesel and light olefins such as ethylene and propylene. It has been well known that FCC catalysts play a pivotal role in determining the feature and efficiency of this process.[1,2] Since the mid-1960s, numerous efforts have been devoted to improving the preparation methods of FCC catalysts and great advances have been achieved.[2–14] Such a progress is the so-called in-situ synthesis technique developed by the former Engelhard Corporation (now acquired by BASF (Badische Anilin- and Soda-Fabrik), Germany). In the in-situ synthesis process, preformed microspheres, obtained by calcining microspheres composed of a mixture of hydrated kaolin, a dispersible boehmite alumina, and a kaolin clay calcined through its characteristic exotherm, undergo chemical reactions with a sodium silicate solution to form crystals of zeolite and a porous silica/alumina matrix.[4–8] Compared with conventional FCC catalysts fabricated by mechanically binding preformed zeolite crystals and kaolin powders with a binder alumina, in-situ synthesized FCC catalysts exhibit extreme stability to steam at high temperature, excellent accessibility of active sites to heavy oil molecules, and higher tolerance capacity to

Correspondence concerning this article should be addressed to X. Bao at baoxj@cup.edu.cn.

contaminant metals and thereby superior catalytic activity. This is because (1) the calcinations at extremely high temperatures during the in-situ synthesis procedure endow the resulting catalysts with a stable, attrition-resistant matrix;[4–6,10,16] (2) the further treatment of microspheres with a caustic solution to leach silica from the particles results in the formation of a network of pore channels along with which the zeolite crystals are grown in-situ, which accounts for the complete zeolite dispersion along the pore walls in the alumina-rich matrix and the growth of an extremely high concentration of zeolites in catalyst; the higher dispersion of the zeolite also gives the high geometric surface area of the zeolite and thus reduces destruction caused by vanadium fluxing, making the catalyst vanadium tolerant;[9–16] (3) growth of zeolite within the microsphere pore structure causes a high degree of interaction between the zeolite and matrix surfaces forming intense chemical bonds, and this matrix-zeolite bond stabilizes the zeolite and makes it extremely resistant to sintering or pore collapse, which is the reason for the outstanding hydrothermal stability;[7–15] and (4) the high surface area alumina matrix, high zeolite dispersion and the easy accessibility of the zeolite are thus responsible for the bottoms upgrading benefits of in-situ synthesized catalysts.[12–19]

While having met widespread commercial success, the in-situ synthesis technique is now confronted with two challenges, i.e., the increasingly heavier feedstocks to FCC units and the ever-fast depletion of high-quality kaolin mineral.[20–22] On one hand, since the early 1980s many refiners have been processing at least a portion of residual oil (resid) as a feedstock of their FCC units, and now nearly all the refiners over the world have to run a full resid catalytic cracking program. It is highly favorable if the catalysts can upgrade resid feedstock, minimize coke and gas formation, maximize catalyst stability, and minimize the deleterious contaminant selectivity due to metal contaminants in resid feedstocks such as nickel and vanadium. This combination of properties presents a challenge to the present in-situ synthesized catalysts. On the other hand, high-quality kaolin minerals used for in-situ FCC catalyst making is in short supply because of the rapid growth of their consumption in paper manufacturing and petrochemical industries.[22,23] Therefore, exploring new natural minerals that provide comparable or even better properties than kaolin for fabricating in-situ catalysts has been a focus of FCC catalyst research and development.

Herein, we report a natural clay mineral rectorite that could replace kaolin for making in-situ FCC catalysts. We demonstrated that the rectorite mineral after being treated at a certain temperature had suitable chemical composition, high chemical reactivity, outstanding stability and thus could be taken as a substitute of kaolin for synthesizing FCC catalysts. Moreover, we had shown that a ZSM-5/rectorite composite consisting of a ZSM-5 layer with a thickness of ca. 6 μm overgrown on preformed rectorite substrate could be successfully synthesized under conventional hydrothermal conditions. Significantly, when used as FCC additive, the obtained ZSM-5/rectorite composite exhibited better catalytic performance for enhancing light olefin yields than the corresponding composite from a commercial kaolin.

Experimental

Raw materials

The natural rectorite mineral containing 90 wt % rectorite used in the present study was purchased from Hubei Celebrities Rectorite Technology (P. R. China). For comparison purpose, a commercial kaolin (containing 95 wt % kaolinite, kindly provided by Lanzhou PetroChemical Company, PetroChina Company) for making in-situ FCC catalysts was also used in the present investigation. Waterglass containing 26.0 wt % SiO_2 and 8.2 wt % Na_2O and tetrapropylammonium bromide (TPABr, 99.0%) were purchased from the market.

Thermal treatment of the clay minerals

To understand the effect of thermal treatment on the properties of the rectorite mineral and thereby to determine the optimum thermal treatment temperature to activate silicon and alumina species for the in-situ synthesis of zeolite, a series of thermally treated rectorite samples were obtained by heating the raw rectorite mineral to different temperatures at a rate of 4°C/min and then maintaining at these temperatures for 2 h in an oven with air recirculation. For comparison, a series of kaolin samples were also thermally treated in parallel under the corresponding treatment conditions.

Measurement of the active Al_2O_3 and SiO_2 contents in thermally treated samples

By definition, active Al_2O_3 and SiO_2 in the calcined samples are those formed during the calcination, leachable by acid or alkali solution, and can contribute all or part of Al and Si species for the in-situ synthesis of zeolite.[24] In the present study, the active Al_2O_3 and SiO_2 contents of the different samples were obtained by first leaching 2 g of a calcined sample with 50 mL of a 4 M HCl solution or with 50 mL of a 4 M NaOH solution at 70°C for 4 h, then filtering and washing the leached sample, and finally analyzing the filtrates by the inductively coupled plasma method conducted on a PE5300DV instrument (Waltham, MA).

In-situ synthesis

First, a mixture consisting of 100 g of calcined mineral (either rectorite or kaolin) powders, 10 mL of a 5 M HNO_3 solution, and appropriate amount of water was prepared, extruded to bars of 1.5 mm in diameter, and calcined at 800°C for 2 h; then, the bars were crushed and sieved to obtain particles of 70–150 μm in size, the resulting particles were referred to as P-Rec-800 and P-Kao-800, where P, Rec, Kao, and 800 denote particle, rectorite, kaolin, and the thermal treatment temperature, respectively; finally, in-situ synthesis of ZSM-5 zeolite on P-Rec-800 and P-Kao-800 was performed as follows: 5 g of P-Rec-800 or P-Kao-800 was added to an aqueous solution (70 mL) containing 1.74 g of TPABr, then 15 g of waterglass was added; after being stirred at room temperature for 30 min, the resulting gel mixture was moved to an autoclave and crystallized at 150°C for 48 h, thus obtained in-situ synthesis products from the calcined rectorite and the calcined kaolin minerals were referred to as AS-Rec-800 and AS-Kao-800, respectively, where AS denote as-synthesized. The further treatment of AS-Rec-800 and AS-Kao-800 in 100% water vapor at 800°C for 4 h yielded two samples denoted by HT-AS-Rec-800 and HT-AS-Kao-800, where HT denotes hydrothermal treatment.

Table 1. Physicochemical Properties of Daqing AR Feed

Items	Daqing AR Feed
Density (20°C) (kg/m^3)	913.00
Kinematic viscosity at 100°C (mm^2/s)	47.43
Carbon residue (wt %)	4.30
Average molecular weight (g/mol)	577
Lumped composition (wt %)	
Saturated alkanes	57.08
Aromatics	27.61
Resins and asphaltenes	15.31
Element composition (wt %)	
C	86.77
H	12.87

The ZSM-5 contents in AS-Rec-800 or AS-Kao-800 were estimated by comparing the integral intensity of the characteristic X-ray diffraction (XRD) peaks of ZSM-5 (2θ at 7.9°, 8.7°, 23.0°, and 23.9°) in the composites to those of a standard ZSM-5 sample using a working curve.[14] The working curve was obtained by plotting the intensity of these ZSM-5 characteristic diffraction peaks vs. the mass fraction of ZSM-5 in a series of mechanical mixtures with known contents of ZSM-5 and Rec-800 or Kao-800.

Characterizations

The phase structure of the samples was characterized by XRD analysis conducted on a Shimadzu 6000 diffractometer (Kyoto, Japan) that uses CuKα radiation and was operated at 40 kV, 30 mA, and 2θ scanning speed of 4°/min. The chemical composition of the two clay samples was determined by X-ray fluorescence (XRF) using a S4 Explorer instrument (Bruker). Thermogravimetry and differential scanning calorimetry (TG-DSC) analyses were performed on a Netzsch STA409PC thermogravimetric analyzer (Netzsch, Germany) at a heating rate of 5°C/min in air. The scanning electron microscopy (SEM) study of the samples was conducted on a Cambridge S-360 apparatus (Cambridge, England) combined with energy-dispersive X-ray spectrometry (EDX). The textual characterization of the different samples was performed by the N_2 adsorption method conducted on a Micromeritics ASAP 2020M system (Micromeritics) at liquid nitrogen temperature. The Brunauer-Emmett-Teller (BET) method was used to calculate the specific surface areas of the samples. The Fourier transformed infrared (FTIR) spectra of the samples were recorded using a Nicolet Magna-IR 560 ESP spectrometer (Nicolet) with a resolution of 1 cm^{-1}.

Catalytic performance assessment

The H-form samples of AS-Rec-800 and AS-Kao-800 were obtained by repeated ion exchanges with a NH_4NO_3 solution of 1.0 M/L and calcination at 500°C for 2 h. The obtained H-form samples were used as FCC additives to enhance light olefin yields. The main FCC catalyst was a composite catalyst consisting of 20 wt % ultrastable Y, 50 wt % kaolin-derived matrix, and 30 wt % alumina binder. The FCC catalysts containing 30 wt % H-form AS-Rec-800 and 30 wt % H-form AS-Kao-800 were referred to as Cat-1 and Cat-2, respectively. Before assessment, Cat-1 and Cat-2 were deactivated with 100% vapor at 800°C for 10 h to simulate the commercial deactivation process.

The catalytic performance assessment tests were carried out on a micro-activity test unit using Daqing atmospheric residue as feedstock whose physicochemical properties are listed in Table 1. The reactions were carried out under the standard conditions: 580°C, feed injection time 20 s, catalyst to oil ratio (mass/mass) 10, water to oil ratio (mass/mass) 1.3, and catalyst loading 50 g. Before each test, the system was purged by a N_2 flow (30 mL/min) for 30 min at reaction temperature. After the feed injection, catalyst stripping was performed using a N_2 flow for 15 min. During the reaction and stripping processes, liquid products were collected in a glass receiver kept in an ice-bath, and the gaseous products were collected in a burette by water displacement. Finally, the gaseous product was analyzed on an Agilent 6890 gas chromatograph installed with a ChemStation software for quantitative determination of light hydrocarbons. The liquid product was analyzed using a simulated distillation gas chromatogram as described in the ASTM D2887 standard. The coke content was determined by a coke analyzer.

In this study, the propylene selectivity was calculated based on the ratio of propylene yield to liquefied petroleum gas yield. The conversion of the feedstock in the reaction process was defined as 100% minus the ratio of the diesel and heavy oil fractions to the feedstock (mass to mass).[25]

To compare the activity stability of the H-form AS-Rec-800 and AS-Kao-800, the catalytic performances of Cat-1 and Cat-2 after three cycles of reaction-regeneration, which were referred to as R-Cat-1 and R-Cat-2, respectively, were also assessed. The regeneration was carried out by calcining Cat-1 and Cat-2 in air at 750°C for 6 h.

Results and Discussion

Chemical composition and structure

Table 2 lists the chemical compositions of the rectorite and kaolin minerals obtained by XRF analysis. It can be seen that both the rectorite and kaolin minerals are mainly composed of Al_2O_3 and SiO_2 and have almost the identical molar SiO_2/Al_2O_3 ratios (1.84 for the rectorite mineral and 1.92 for the kaolin mineral). This suggests that like the kaolin mineral, the rectorite mineral can also provide enough active Al_2O_3 and SiO_2 as raw materials for the in-situ crystallization of zeolite. It should be noted that the Al_2O_3 and SiO_2 contents of the rectorite mineral are slightly lower, whereas the contents of other metal ions, such as Na^+, Ca^{2+}, K^+, etc., are relatively higher than those in the commercial kaolin mineral. This is not only because of the relatively

Table 2. Chemical Compositions of the Kaolin mineral and Rectorite Minerals

Component (wt %)	Na_2O	Al_2O_3	SiO_2	P_2O_5	SO_3	MgO	K_2O	CaO	TiO_2	Fe_2O_3	ZrO_2
Kaolin	2.8	44.6	50.5	0.2	0.3	0.1	0.4	0.1	0.3	0.5	–
Rectorite	1.3	38.2	41.3	0.4	2.9	0.5	1.9	7.2	3.8	2.1	0.1

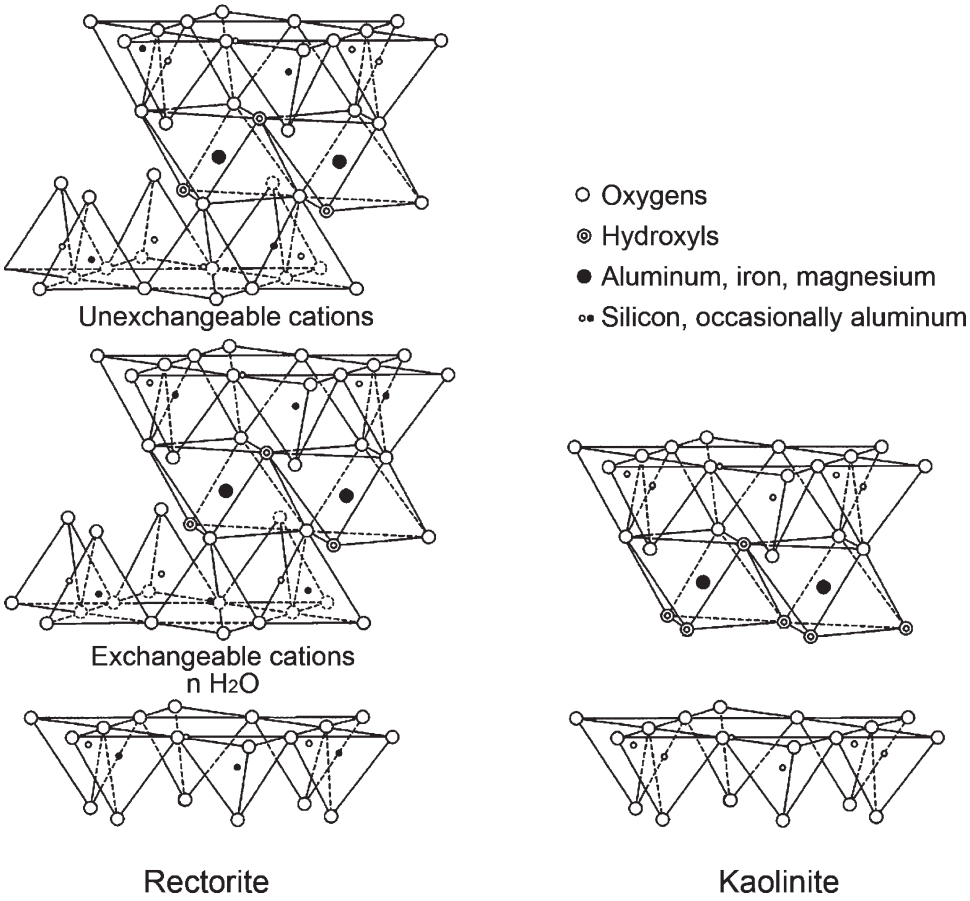

Figure 1. Schematic illustration of the framework structures of rectorite and kaolinite.

lower grade (90 wt %) of the rectorite mineral than that of the kaolin mineral (95 wt %), but also because of the more complicated structure of the former than the latter.

Figure 1 schematically illustrates the framework structures of rectorite and kaolinite.[26–28] As seen, rectorite consists of a regular 1:1 stacking of mica- and smectite-like layers, and both mica- and smectite-like layers have lattice structure in which two-dimensional oxyanions are separated by layers of cations. In either mica- or smectite-like layers, the oxygen atoms define upper and lower sheets of tetrahedral sites and a central sheet of octahedral sites. The 2:1 relation between the tetrahedral and octahedral sheets allows both mica- and smectite-type clays to be classified as 2:1 phyllosilicates. This structural designation differentiates rectorite from 1:1 clay minerals such as kaolinite whose layers are formed by coupling only one tetrahedral sheet with one octahedral sheet.

The cations on the interlamellar surfaces of both the mica- and smectite-like layers in rectorite balance the negative charge deficiency of framework which results from the substitution of Si^{4+} by Al^{3+} in tetrahedral positions or from the substitution of Al^{3+} by Mg^{2+} in octahedral positions. Particularly, the cations of the smectite-like layers are hydrated and exchangeable, leading to the intercalation and swelling properties of rectorite. The cations of mica-like layers have no exchangeable capacity, but the existence of these mica-like layers improves the structure stability of rectorite. For the structure of kaolinite, however, there is very little substitution in structure lattices and thus it has almost no interlayer cations.

The above structure analysis clearly shows why rectorite has much more other metal ions than kaolinite. Most importantly, the complicated structure of rectorite result in its unique properties, including outstanding thermal and hydrothermal stabilities, swelling property, cation exchange capacity, and intercalation property. It is these outstanding properties that have kindled interests using rectorite as catalyst or catalyst support in recent years.[27]

Thermal properties

The thermal properties of kaolinite are essential to the in-situ synthesis technique, and for this reason we investigated the thermal behavior of the rectorite and kaolin minerals in parallel by means of TG-DSC and XRD, and the pretreatment conditions of rectorite for in-situ synthesis were determined.

Figure 2 shows the TG-DSC curves of the rectorite and kaolin minerals. From Figure 2A, it can be seen that the TG-DSC curves of the rectorite can be divided into the following three regions: (1) the region below 400°C, in which the two endothermic peaks at 100°C and 160°C on the DSC curve can be assigned to the losses of adsorbed and interlayer water, respectively, and the weight loss in this region

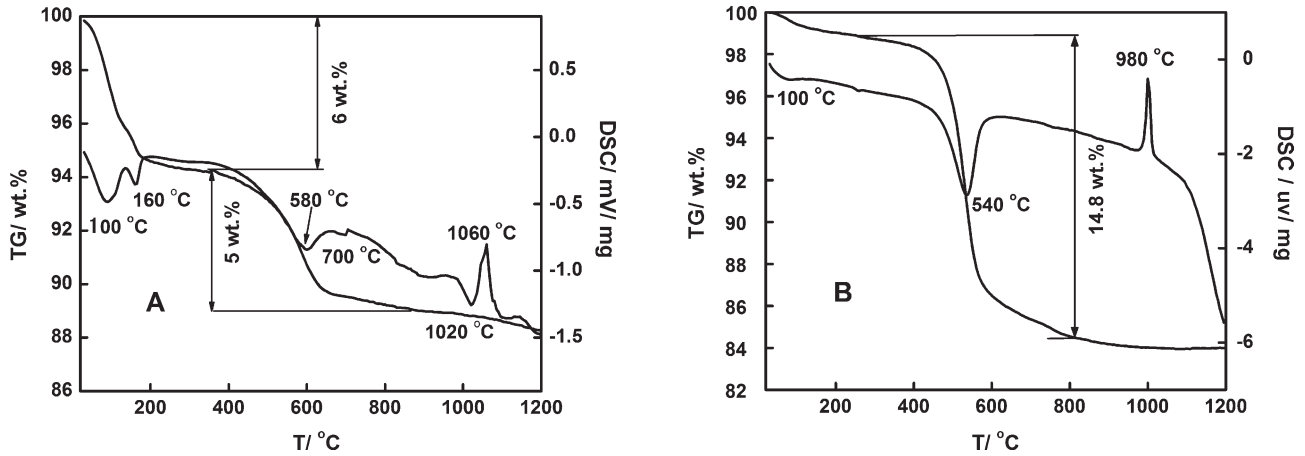

Figure 2. DSC and TG curves of the rectorite (A) and kaolin (B) minerals.

was estimated about 6 wt % from the corresponding TG curve; (2) the region between 400°C and 1000°C, in which there are two endothermic peaks at 580°C and 700°C, attributed to the dehydroxylation of smectite-type layers and mica-like layers of the rectorite, respectively,[29] and the weight loss of the rectorite is about 5 wt %; (3) the region above 1000°C, in which the endothermic peak at 1020°C and the followed exothermal peak at 1060°C reflect the destruction of the rectorite and the formation of new phases, respectively. For the kaolin mineral, the TG-DSC curves in Figure 2B can also be divided into three different regions: (1) the region below 400°C, in which the endothermic peak at 100°C is assigned to the removal of adsorbed water; (2) the region between 400°C and 900°C, in which the dehydroxylation of kaolinite occurs, with a 14.8 wt % weight loss as shown by the TG curve; (3) the region above 900°C, in which the characteristic exothermal peak at 980°C indicates the decomposition of kaolinite structure and the formation of more stable phases. By comparing the TG-DSC profiles, we can observe that the two clay minerals have distinctively different thermal behaviors, suggesting that their activation pretreatments for in-situ synthesis should be therefore different, which we will discuss later in more detail. We also note that the dehydroxylation of the rectorite shows lower endothermic peaks with less weight losses than those of the kaolin mineral, indicating the slighter structure change of the former. Significantly, the higher exothermal temperature of the rectorite mineral representing the formation of new phases than that of the kaolin mineral further demonstrates the excellent structure stability of the rectorite mineral.

Figure 3 shows the XRD patterns of the rectorite and kaolin minerals and their thermally treated products. As shown in Figure 3A, the rectorite phase in the rectorite sample is well maintained even after the dehydroxylation process, in agreement with the TG-DSC results discussed above. After being calcined at 1000°C, the thermally treated rectorite shows a very low crystallinity, suggesting the decomposition of the crystalline structure; as a consequence, amorphous SiO_2 and Al_2O_3 are formed. The calcination at 1100°C resulted in the appearance of the new stable phases mullite and cristobalite. As shown in Figure 3B, kaolinite lost its characteristic peaks after being calcined at temperature ranging from 600°C to 900°C, showing only an amorphous band assigned to a highly disordered phase with high chemical reactivity, metakaolinite.[30,31] In the XRD pattern of the kaolin sample calcined at 1000°C, the characteristic peaks of Si–Al spinel appeared, whereas further increasing the calcination temperature to 1200°C resulted in the formation of a new phase mullite.

By combining the TG-DSC and XRD results above, the chemical reactions representing the phase transformations of the rectorite and kaolin minerals during the calcination process can be summarized by Formulae 1 and 2, respectively. In Formulae (1) and (2), M indicates metal cations.

$$\begin{cases} MAl_8Si_8O_{20}(OH)_4 \cdot nH_2O(\text{rectorite}) \xrightarrow{\sim 700^oC} MAl_8Si_8O_{22} + 2H_2O \\ Mal_4Si_8O_{22} \xrightarrow{\sim 1020^oC} Al_2O_3(\text{amorphous}) + SiO_2(\text{amorphous}) \\ Al_2O_3 + SiO_2 \xrightarrow{\sim 1060^oC} Si_2Al_6O_{13}(\text{mullite}) + SiO_2(\text{cristobalite}) \end{cases} \quad (1)$$

$$\begin{cases} Al_2O_3 \cdot 2SiO_2 \cdot 2H_2O(\text{kaolinite}) \xrightarrow{\sim 600^oC} Al_2O_3 \cdot 2SiO_2(\text{metakaolin}) + 2H_2O \\ Si_2Al_2O_7 \xrightarrow{\sim 980^oC} Si_3Al_4O_{12}(\text{spinel}) + SiO_2(\text{amorphous}) \\ Si_3Al_4O_{12}(\text{spinel}) \xrightarrow{\sim 1100^oC} Si_2Al_6O_{13}(\text{mullite}) \end{cases} \quad (2)$$

As shown in Formulae (1) and (2), the calcination of the rectorite and kaolin minerals at suitable temperatures leads to the formation of amorphous Al_2O_3 and SiO_2 that are leachable by acid and alkali, respectively, and thus can contribute all or part of Al or/and Si species for zeolite synthesis. To search for optimum temperatures for activating Al_2O_3 and SiO_2 in the two clay minerals, the contents of active Al_2O_3 and SiO_2 in the calcined products vs. calcination temperature were investigated and the results are shown in Figure 4. For both of the two clay minerals, the contents of active Al_2O_3 and SiO_2 first increase with the increasing calcination temperature, then reach their maxima, and finally decrease with the increasing calcination temperature. This can be well explained from Formulae (1) and (2): with the increasing calcination temperature, more amorphous SiO_2 and Al_2O_3 are formed; when the calcination temperature

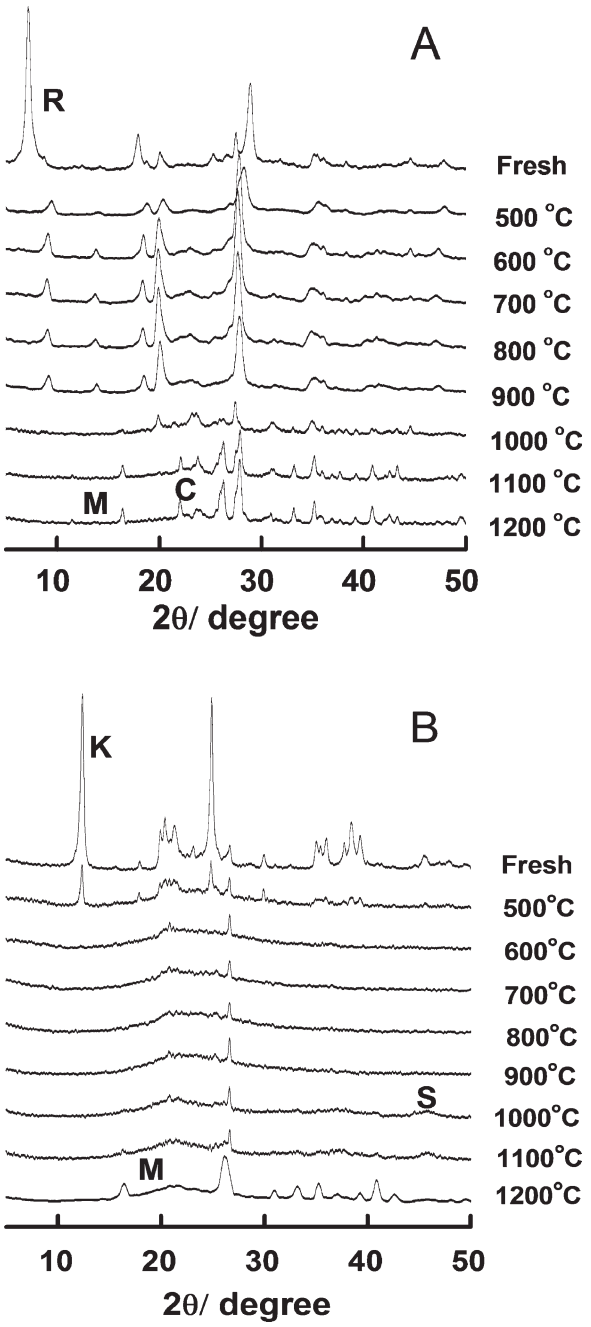

Figure 3. XRD patterns of the rectorite (A) and kaolin (B) samples thermally treated at different temperatures.

R, M, C, K, and S denote rectorite, mullite, cristobalite, kaolinite, and spinel, respectively.

exceeds a certain value, the formed SiO_2 and Al_2O_3 recombine to form mullite and cristobalite (for the rectorite) or mullite (for the kaolin), resulting in the decreased contents of active SiO_2 and Al_2O_3. It also comes to our notice that for the kaolin mineral, the contents of amorphous Al_2O_3 and SiO_2 reach maxima simultaneously when the calcination temperature is in the range of 1000–1100°C; whereas for the kaolin mineral, the calcination temperatures for obtaining maximum contents of Al_2O_3 and SiO_2 appear at about 800°C and 1000°C, respectively. Such a difference for the two minerals can be also well understood from Formulae (1) and (2).

The different thermal activation behaviors of the two minerals may lead to different thermal pretreatments when they are used for in-situ synthesis. To overcome the problem of the different temperatures for achieving maximum active SiO_2 and Al_2O_3 contents in activating kaolin, two kaolin products calcined at two different temperatures must be involved in industrial practice,[8] with one being calcined at lower temperature ranging from 600°C to 980°C, mainly containing metakaolinite and exhibiting high chemical activity, but lacking structural stability,[6] and the other being thermally treated at temperature above 980°C and mainly containing the stable spinel phase which serves as a stable porous matrix after alkali leaching during the hydrothermal synthesis.[10] For the rectorite mineral, however, the calcination temperatures for achieving maximum active SiO_2 and Al_2O_3 contents are almost the same, which excludes the necessity to use two different calcination temperatures and thus provides a simpler and more economical route for the in-situ synthesis of high performance FCC catalysts.

From the above results, it can be concluded that the rectorite can be effectively activated by calcination at temperature ranging from 800°C to 1200°C. In addition, considering the higher stability of rectorite, the thermal activation of rectorite for in-situ synthesis purpose should be carried out in the temperature range of 800–1000°C. In the present study, we used a rectorite sample calcined at 800°C for in-situ synthesis.

In-situ synthesis

To demonstrate the feasibility of rectorite to replace kaolin for making FCC catalysts, the in-situ synthesis experiment using P-Rec-800 as the starting material was performed under the conventional hydrothermal conditions and compared with that using P-Kao-800, and the SEM micrographs of the resulting in-situ synthesis products denoted by AS-Rec-800 and AS-Kao-800, respectively, are shown in Figure 5. It can be seen that the outer surfaces of the two products are closely packed with uniform cubic crystals of ca. 2 μm in size. The XRD patterns of the resulting composites in Figure 6 show that these crystal materials are zeolite ZSM-5. Further EDX analyses demonstrate that the molar SiO_2/Al_2O_3 ratios of ZSM-5 crystals in AS-Rec-800 and AS-Kao-800 are 52.3 and 59.2, respectively. Undoubtedly, the Al species in the framework of in-situ crystallized ZSM-5 crystals come from the calcined rectorite and kaolin because they are the only alumina sources in the in-situ synthesis system. This indicates that like the calcined kaolin, the calcined rectorite can also contribute active Al_2O_3 and SiO_2 to the in-situ synthesis of ZSM-5, although most Si species in the synthesized ZSM-5 comes from the added waterglass.

The crystallization of ZSM-5 resulted in dramatic changes in the textual properties of the substrates. As seen in Table 3, P-Rec-800 and P-Kao-800 that were used as raw materials are both calcined particles with their BET surface areas at 6.2 and 4.3 m^2/g and pore volumes at 0.07 and 0.06 cm^3/g, respectively, whereas the in-situ synthesis products AS-Rec-800 and AS-Kao-800 have BET surface areas and pore volumes as high as 126.2 and 112.3 m^2/g and 0.13 and 0.12 cm^3/g, respectively. The increased surface areas and pore volumes of the in-situ synthesis products AS-Rec-800 and

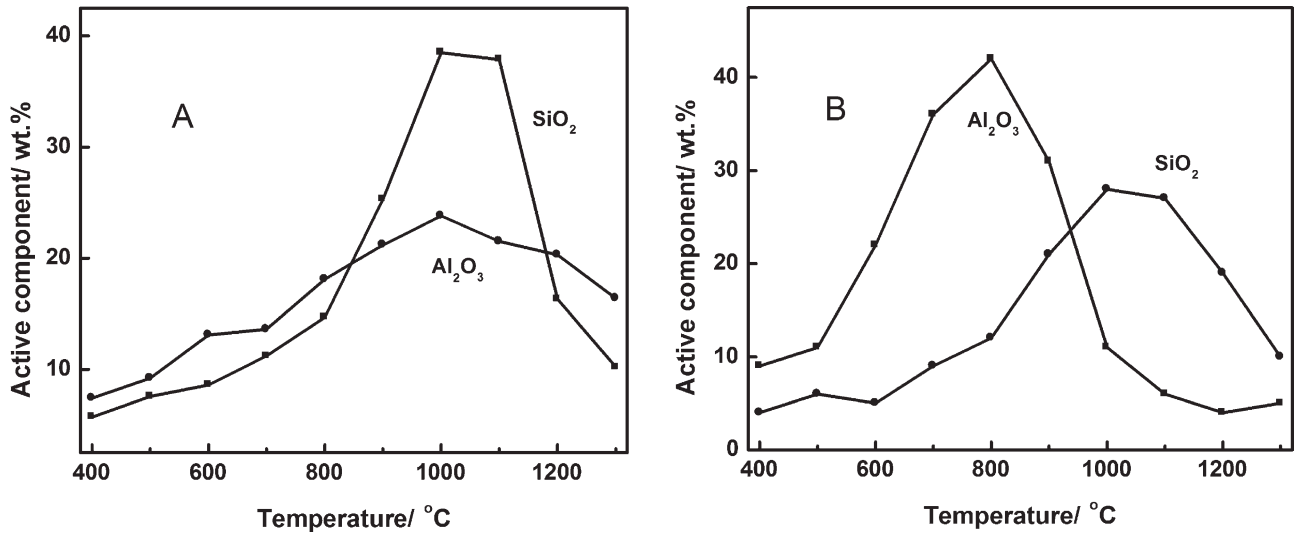

Figure 4. Relationship between the contents of active SiO_2 and Al_2O_3 and the activation temperature for the calcined rectorite (A) and kaolin (B) samples.

AS-Kao-800 are attributed to the dissolving of activated SiO_2 and Al_2O_3 from the substrates by the alkali medium and the overgrowth of microporous ZSM-5 along the network of pore channels created in the substrates by alkali leaching.[32]

By using the working curve aforementioned, the contents of ZSM-5 in AS-Rec-800 and AS-Kao-800 were estimated to be 34.6 wt % and 31.5 wt %, respectively. After the hydrothermal treatment in 100% vapor at 800°C for 2 h, the ZSM-5 content in HT-AS-Rec-800 (the hydrothermally treated sample of AS-Rec-800) was lowered to 30.3 wt %, much higher than 24.1 wt % of HT-AS-Kao-800 (the hydrothermally treated sample of AS-Kao-800). The well maintained ZSM-5 crystallinity in AS-Rec-800 after the hydrothermal treatment demonstrates its much better hydrothermal stability. The superior hydrothermal stability of AS-Rec-800 was further confirmed by measuring its textual properties before and after the hydrothermal treatment. As shown in Table 3, the HT-AS-Rec-800 could well maintain its BET surface area, particularly the microporous BET surface area due to ZSM-5. The excellent structural stability of AS-Rec-800 should be attributed to the superior structure stability of the rectorite phase in the composite. Even after the in-situ synthesis process, the rectorite phase in the composite can be still distinguished, as shown by the XRD patterns of AS-Rec-800 in Figure 6. This result is in good agreement with literature report.[2]

Figure 7 shows the FTIR spectra of P-Rec-800 and P-Kao-800, two mechanical mixtures Rec-800/ZSM-5 (containing 30 wt % ZSM-5) and Kao-800/ZSM-5 (containing 30 wt % ZSM-5), and the resulting in-situ products AS-Rec-800 and AS-Kao-800. For all the samples, the band at the wave number of about 1640 cm^{-1} arising from water adsorbed from the environment was observed. For the samples P-Rec-800 and P-Kao-800, the characteristic bands of P-Rec-800 at about 1042, 877, 686, 560, and 480 cm^{-1} on curve (A) in

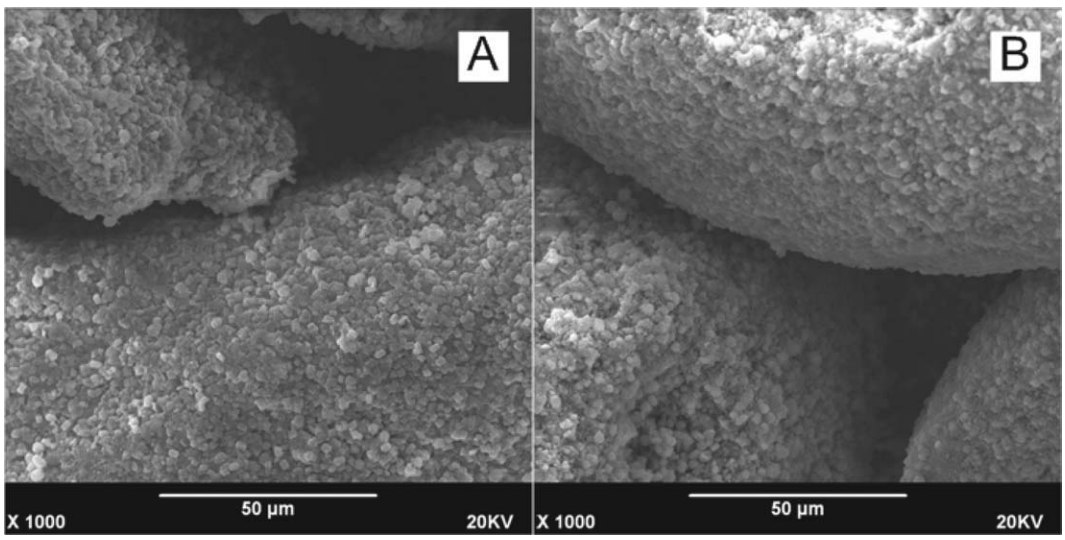

Figure 5. SEM images of the in-situ synthesized products (A) AS-Rec-800 and (B) AS-Kao-800.

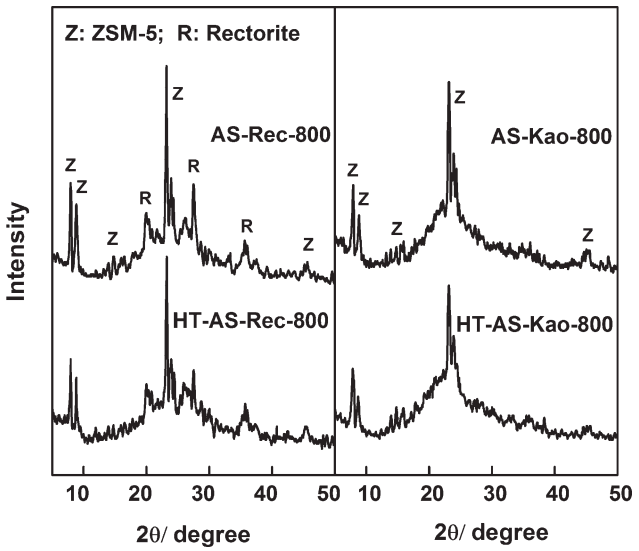

Figure 6. XRD patterns of the in-situ synthesized composites AS-Rec-800 and AS-Kao-800 and the hydrothermally treated products HT-AS-Rec-800 and HT-AS-Kao-800.

Figure 7 are assigned to Si—O—Si stretching, Al—O—(H) libration, Si—O—Al bending, Si—O—Al bending and Si—O bending in rectorite structure, respectively[33]; while the bands at 1090, 815, and 475 cm^{-1} on curve (D) in Figure 7 are due to the vibrations of SiO_4, AlO_4, and SiO_4 tetrahedra in P-Kao-800.[32] Compared with literature results,[32,33] most of the characteristic bands assigned to rectorite structure can be clearly seen in the FTIR spectra of P-Rec-800, whereas most of the characteristic bands assigned to kaolinite structure vanished in the FTIR spectra of P-Kao-800, indicating the much higher structural stabilities of rectorite than kaolinite. This result is in accordance with those of above thermal behavior analysis. In the spectra of the two mechanical mixtures Rec-800/ZSM-5 [curve (B) in Figure 7] and Kao-800/ZSM-5 [curve (E) in Figure 7], we can observe two more bands located at 545 and 1222 cm^{-1} assigned to the five-membered rings of the pentasil zeolite structure and the external Si—O—Si (Si—O—Al) linkages of ZSM-5, respectively, in addition to those appearing in the spectra of Rec-800 and Kao-800.[34–36] In the spectra of AS-Rec-800, it is interesting to note that several new bands that are assigned to ZSM-5 at about 545 and 1222 cm^{-1} appeared, and the band assigned to Si—O—Si stretching band at about 1090 cm^{-1} was well maintained, but the bands characteristic to P-Rec-800 such as those at about 877, 686, and 480 cm^{-1} vanished. This suggests that during the in-situ synthesis process the significant changes took place in the chemical environment of Si and Al species on the surface of the rectorite substrate,[31,32] more exactly, the resulting AS-Rec-800 is not a mechanical mixture of the rectorite substrate and ZSM-5 but a composite of the rectorite substrate and ZSM-5 linked by chemical bonding.[37,38] Unlike the samples related to the rectorite, no obvious difference was observed between the FTIR spectra of AS-Kao-800 [curve (F) in Figure 7] and Kao-800/ZSM-5 [curve (E) in Figure 7]. This can be explained by the fact the lower structural stability of kaolinite than rectorite leads to the disappearance of most characteristic band in the calcinations procedure and therefore after the in-situ synthesis only the new bands assigned to the ZSM-5 phase overgrown on the substrate appeared.

The SEM-EDX analysis results of the composite AS-Rec-800 are shown in Figure 8. From Figure 8A, we can see that the outer surface of AS-Rec-800 is uniformly covered with cubic ZSM-5 crystals of ca. 2 μm in size, in coincidence with the results shown in Figure 5A. By sectioning an AS-Rec-800 particle, two textural regions with different color depth can be easily distinguished: the core region being the P-Rec-800 substrate and the shell region being a layer of zeolite ZSM-5 crystals with thickness ca. 6 μm. Significantly, we found that no clear interface but a transitional area exists between the two regions, demonstrating that AS-Rec-800 is a composite consisting of in-situ crystallized zeolite ZSM-5 crystals chemically bonded to the inner substrate rather than a mechanical mixture of Rec-800 and ZSM-5,[9] in accordance with the above FTIR analysis results. To further confirm this, the molar SiO_2/Al_2O_3 ratios of six micro-areas (marked by a, b, c, d, e, and f in Figure 8B) selected on the transverse section were analyzed by EDX and the results are shown in Figure 8C. By glancing at the figure, we can see that the molar SiO_2/Al_2O_3 gradually decreases from the outer layer to the inner core of the composite, with the outer ZSM-5 shell having a molar SiO_2/Al_2O_3 ratio of about 50 and the core region having a molar SiO_2/Al_2O_3 ratio of about 1.9 which is almost identical to that of the rectorite mineral. Most significantly, it is found that the molar SiO_2/Al_2O_3 ratio smoothly changes across the interface between the ZSM-5 film and the P-Rec-800 substrate, fully demonstrating the composite nature of AS-Rec-800.

By combining the above SEM and EDX analysis results, we can conclude that the in-situ crystallization product AS-Rec-800 of P-Rec-800 is a composite consisting of a layer of ZSM-5 of ca. 6 μm in thickness as shell and the unreacted P-Rec-800 as core.

Catalytic performance assessment results

The catalytic performance of the rectorite-derived in-situ crystallization product AS-Rec-800 in its H-form as FCC additive for boosting light olefin yields was tested and the results are listed in Table 4, in which the reaction results of the kaolin-derived in-situ crystallization product AS-Kao-800 in its H-form and the two catalysts (R-Cat-1 and R-Cat-2) regenerated after three reaction-regeneration cycles are also included for comparison purpose. It can be seen that, at the

Table 3. Textual Properties of the Rectorite and Kaolin–Derived Samples

Comparing Samples	S_{BET} (m^2/g)	S_{Mic} (m^2/g)	S_{Ext} (m^2/g)	V_P (cm^3/g)
P-Rec-800/ P-Kao-800	6.2/4.3		6.2/4.3	0.07/0.06
AS-Rec-800/AS-Kao-800	126.2/112.3	114.1/103.8	12.1/ 8.5	0.13/0.12
HT-AS-rec-800/ HT-AS-Kao-800	119.7/81.4	107.3/70.9	12.4/10.5	0.13/0.11

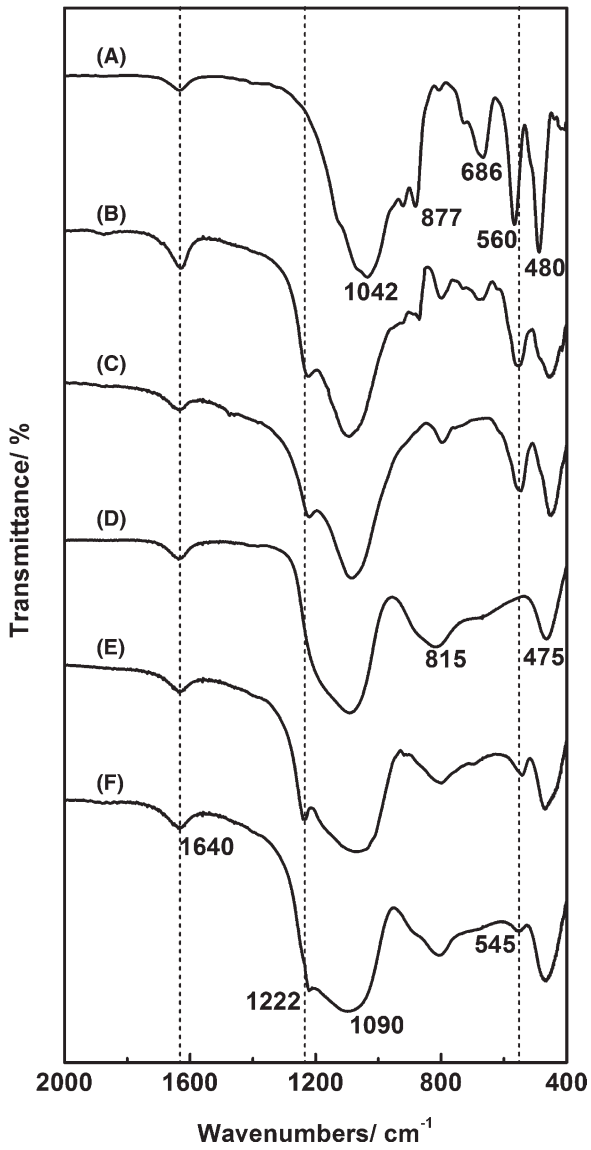

Figure 7. FTIR spectra of the raw material P-Rec-800 (A), the mechanical mixture Rec-800/ZSM-5 (B), the resulting composite AS-Rec-800 (C), the raw material P-Kao-800 (D), the mechanical mixture Kao-800/ZSM-5 (E), and the resulting composite AS-Rec-800 (F).

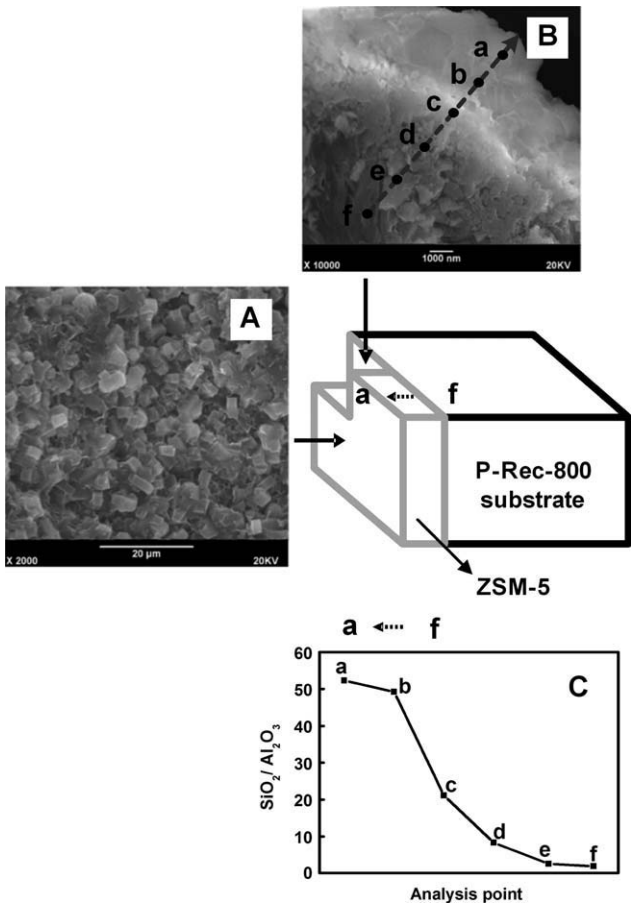

Figure 8. SEM and EDX analysis results of the composite AS-Rec-800.

Shown are the SEM image of the outer surface (A) of the polycrystalline zeolite ZSM-5 film overgrown on the P-Rec-800 substrate, the cross-sectional view (B) of a ZSM-5/rectorite particle, and the changing trend of the molar SiO_2/Al_2O_3 ratio of the composite on the transverse section (C).

almost equivalent conversion, the ethylene yield (3.32 wt %), the propylene yield (13.69 wt %) and selectivity (36.33%) obtained on Cat-1 consisting of 30 wt % AS-Rec-800 in H-form and 70 wt % model FCC catalyst are higher than those (3.17 wt %, 13.02 wt %, and 35.33%) over Cat-2 consisting of 30 wt % AS-Kao-800 in H-form and 70 wt % model FCC catalyst. Significantly, after three reaction-regeneration cycles, R-Cat-1 still keeps its higher ethylene yield (3.26 wt %), propylene yield (13.38 wt %) and selectivity (36.14%), but R-Cat-2 gives obviously decreased light olefin yields (3.07 wt % for ethylene and 12.42 wt % for propylene). These results demonstrate the better light olefin boosting performance of the FCC additive derived from rectorite than that from kaolinite, attributed to the outstanding textual and structural stability of the in-situ synthesized product AS-Rec-800 of the rectorite mineral.

Table 4. Catalytic Cracking Results over the Different Catalysts

	Catalysts			
	Cat-1	Cat-2	R-Cat-1	R-Cat-2
Product yields (wt %)				
Dry gas	6.44	6.09	6.25	5.87
LPG	37.68	36.85	37.02	35.24
Gasoline	29.27	30.58	30.23	32.08
Diesel	14.97	15.08	14.82	15.21
Heavy oil	7.52	7.49	7.65	7.44
Coke	4.12	3.91	4.03	4.16
Ethylene	3.32	3.17	3.26	3.07
Propylene	13.69	13.02	13.38	12.42
Ethylene + propylene	17.01	16.19	16.64	15.49
Propylene selectivity (%)	36.33	35.33	36.14	35.24
Conversion (wt %)	77.51	77.43	77.53	77.35

Conclusions

The potential of using a natural aluminosilicate mineral rectorite as raw material for the in-situ synthesis of FCC catalysts was explored in this investigation. By comparing the properties of a raw rectorite mineral and a raw kaolin mineral, their calcination products, and their in-situ synthesis products, we have shown that the rectorite mineral has suitable chemical composition, outstanding stability, and enough chemical reactivity after thermal activation in the temperature range from 800°C to 1000°C and thus could be taken as an alternative of kaolin for the in-situ synthesis of FCC catalysts. Furthermore, a core-shell type ZSM-5/rectorite composite was successfully synthesized using the activated rectorite as the starting material. The XRD, BET, FTIR, SEM, and EDX characterization results revealed that the ZSM-5 phase in the composite was present in a film of ca. 6 μm in thickness overgrown on the rectorite substrate. The in-situ synthesized composite from the rectorite mineral demonstrated excellent catalytic performances for enhancing light olefin yield when used as a FCC additive. These results indicated that rectorite could be used as an alternative feedstock for fabricating high-performance FCC catalysts via the so-called in-situ synthesis route.

Acknowledgments

The authors gratefully acknowledge the financial support by the Ministry of Science and Technology of China through the National Basic Research Program (Grant No. 2010CB226905) and the National Natural Science Foundation of China for the Youth (Grant No. 20706059) and National Science Fund for Distinguished Young Scholars (Grant No. 20825621).

Literature Cited

1. O'Connor P, Imhof P, Yanik SJ. Catalyst assembly technology in FCC. Part 1: a review of the concept, history and developments. In: Occelli ML, O'Connor P, editors. *Stud Surf Sci Catal*. Amsterdam: Elsevier, 2001;134:299–310.
2. Corma A. From microporous to mesoporous molecular sieve materials and their use in catalysis. *Chem Rev*. 1997;97:2373–2420.
3. Corma A. State of the art and future challenges of zeolites as catalysts. *J Catal*. 2003;206:298–312.
4. Haden WL, Dzierzanowski FJ. *Synthetic zeolite contact masses and method for making the same*. U.S. Patent 3 367 886; 1966.
5. Haden WL, Dzierzanowski FJ. *Method for making a faujasite-tape crystalline zeolite*. U.S. Patent 3 338 672 1967.
6. Haden WL, Dzierzanowski FJ. *Solid catalysts*. U.S. Patent 3 367 887; 1968.
7. Basaldella EI, Bonetto R, Tara JC. Synthesis of NaY zeolite on preformed kaolinite spheres. Evolution of zeolite content and textural properties with the reaction time. *Ind Eng Chem Res*. 1993;32:751–752.
8. Haden WL, Dzierzanowski FJ. Microspherical zeolitic molecular sieve composite catalyst and preparation thereof. U.S. Patent 3 647 718; 1972.
9. Tan Q, Bao X, Song T, Fan Y, Shi G, Shen B, Liu C, Gao X. Synthesis, characterization, and catalytic properties of hydrothermally stable macro-meso-micro–porous composite materials synthesized via in situ assembly of preformed zeolite Y nanoclusters on kaolin. *J Catal*. 2007;251:69–79.
10. Lussier RJ, Surland GJ. *Catalysts and catalyst supports*. U.S. Patent 4 749 672; 1988.
11. Degnan TF, Chitnis GK, Schipper PH. History of ZSM-5 fluid catalytic cracking additive development at Mobil. *Micropor Mesopor Mater*. 2000;35–36:245–252.
12. Tan Q, Bao X, Fan Y, Liu H, Song T, Shi G, Shen B. Bimodal micro-mesoporous aluminosilicates for heavy oil cracking: porosity tuning and catalytic properties. *AIChE J*. 2008;54:1850–1859.
13. Lin X, Chen X, Kita H, Okamoto K. Synthesis of silicalite tubular membranes by in situ crystallization. *AIChE J*. 2003;49:237–247.
14. Liu H, Bao X, Wei W, Shi G. Synthesis and characterization of kaolin/NaY/MCM-41 composites. *Micropor Mesopor Mater*. 2003;66: 117–125.
15. Stockwell DM, Brown RP, Brown SH. *Structurally enhanced cracking catalysts*. U.S. Patent 6 656 347; 2003.
16. Xu M, Cheng M, Bao X. Growth of ultrafine zeolite Y crystals on metakaolin microspheres. *Chem Commun*. 2000;1873–1874.
17. Mohamed MM, Zidan FI, Thabet M. Synthesis of ZSM-5 zeolite from rice husk ash: Characterization and implications for photocatalytic degradation catalysts. *Micropor Mesopor Mater*. 2008;108:193–203.
18. Davis ME. Ordered porous materials for emerging applications. *Nature*. 2002;417:813–821.
19. Wang Y, Jin G, Guo X. Growth of ZSM-5 coating on biomorphic porous silicon carbide derived from durra. *Micropor Mesopor Mater*. 2009;118:302–306.
20. Rana MS, Sámano V, Ancheyta J, Diaz JAI. A review of recent advances on process technologies for upgrading of heavy oils and residua. *Fuel*. 2007;86:1216–1231.
21. Puente GDL, Devard A, Sedran U. Conversion of residual feedstocks in FCC. Evaluation of feedstock reactivity and product distributions in the laboratory. *Energy Fuels*. 2007;21:3090–3094.
22. Robert LV. *Mineral Commodity Summaries*. U.S. Geological Survey, US Bureau of Mines, 2008, Washington, DC.
23. Robert LV. *Mineral Commodity Summaries*. U.S. Geological Survey, US Bureau of Mines, 2009, Washington, DC.
24. Zheng S, Sun S, Wang Z, Gao X, Xu X. Suzhou kaolin as a FCC catalyst. *Clay Miner*. 2005;40:303–310.
25. Zhao X, Harding RH. ZSM-5 additive in fluid catalytic cracking. 2. Effect of hydrogen transfer characteristics of the base cracking catalysts and feedstocks. *Ind Eng Chem Res*. 1999;38:3854–3859.
26. Pinnavaia TJ. Intercalated clay catalysts. *Science*. 1983;22:365–371.
27. Occelli ML, Gould SAC. Examination of coked surfaces of pillared rectorite catalysts with the atomic force microscope. *J Catal*. 2001;198:41–46.
28. White CE, Provis JL, Riley DP, Kearley GJ, Van Deventer JSJ. What is the structure of kaolinite? Reconciling theory and experiment. *J Phys Chem B*. 2009;113:6756–6765.
29. Benincasa E, Brigatti MF, Medici L, Poppi L. K-rich rectorite from kaolinized micaschist of the Sesia-Lanzo zone, Italy. *Clay Miner*. 2001;36:421–433.
30. Liu Y, Pinnavaia TJ. Metakaolin as a reagent for the assembly of mesoporous aluminosilicates with hexagonal, cubic and wormhole framework structures from proto-faujasitic nanoclusters. *J Mater Chem*. 2004;14:3416–3420.
31. Youssef H, Ibrahim D, Komarneni S. Microwave-assisted versus conventional synthesis of zeolite A from metakaolinite. *Micropor Mesopor Mater*. 2008;115:527–534.
32. Alkan M, Hopa Ç, Yilmaz Z, Güler H. The effect of alkali concentration and solid/liquid ratio on the hydrothermal synthesis of zeolite NaA from natural kaolinite. *Micropor Mesopor Mater*. 2005;86:176–184.
33. Kloprogge JT, Frost RL, Hickey L. Infrared absorption and emission study of synthetic mica-montmorillonite in comparison to rectorite, beidellite and paragonite. *J Mater Sci Lett*. 1999;18:1921–1923.
34. Campos AA, Dimitrov L, Da Silva CR, Wallau M, Urquieta-González EA. Recrystallisation of mesoporous SBA-15 into microporous ZSM-5. *Micropor Mesopor Mater*. 2006;95:92–103.
35. Kirschhock CEA, Ravishankar R, Verspeurt F, Grobet PJ, Jacobs PA, Martens JA. Identification of precursor species in the formation of MFI zeolite in the TPAOH-TEOS-H_2O system. *J Phys Chem B*. 1999;103:4965–4971.
36. Cheng Y, Wang L, Li J, Yang Y, Sun X. Preparation and characterization of nanosized ZSM-5 zeolites in the absence of organic template. *Mater Lett*. 2005;60:3427–3430.
37. Katsuki H, Furuta S, Komarneni S. Formation of novel ZSM-5/porous mullite composite from sintered kaolin honeycomb by hydrothermal reaction. *J Am Ceram Soc*. 2000;83:1093–1097.
38. Komarneni S, Katsuki H, Furuta S. Novel honeycomb structure: a microporous ZSM-5 and macroporous mullite composite. *J Mater Chem*. 1998;8:2327–2329.

Manuscript received Oct. 3, 2009, and revision received Jan. 18, 2010.